Wind Farm Modeling and Control Using Dynamic Mode Decomposition

Jennifer Annoni*, Joseph Nichols,†, Peter Seiler‡
Department of Aerospace Engineering & Mechanics
University of Minnesota, Minneapolis, MN, 55455, USA

The objective of this paper is to construct a low-order model of a wind farm that can be used for control design and analysis. There is a potential to use wind farm control to increase power and reduce overall structural loads by properly coordinating the turbines in a wind farm. To perform control design and analysis, a model of the wind farm needs to be constructed that has low computational complexity, but retains the necessary dynamics. This paper uses an extension of dynamic mode decomposition (DMD) to extract the dominant spatial and temporal information from computational fluid dynamic simulations. Specifically, this extension of DMD includes input/output information and relies on techniques from the subspace identification literature. Using this information, a low-order model of a wind farm is constructed that can be used for control design.

Nomenclature

A	Rotor Area, $[m^2]$
β	Pitch angle, $[rad]$
C_p	Power coefficient, [unitless]
P	Power captured by the turbine, $[W]$
ρ	Air density, $[kg/m^3]$
u	Wind speed, $[m/s]$
R	Rotor radius, $[m]$
λ	Tip-speed ratio, [unitless]

I. Introduction

In the United States, many states have a Renewable Portfolio Standard (RPS) or Goal. For example, Minnesota has a RPS target of 25% renewable energy by 2025.[1] Wind energy will be a significant factor in achieving this goal. Wind farm control can be used to increase wind energy efficiency by maximizing power in wind farms that are already installed. In can also be used to mitigate structural loads to maximize the lifetime of the turbines and better integrate wind energy into the energy market.

Currently, turbines in a wind farm are operated to maximize their own performance. Many studies have been done showing that operating all turbines at their optimal operating point leads to sub-optimal performance. Properly coordinating turbines in a wind farm has the potential to increase the overall performance of a wind farm.[2] Designing wind farm control strategies requires a model of the wind farm that has low computational complexity, but retains the necessary dynamics. A variety of wake models exist in the literature that are useful for studying wind farm control. The simplest models are the Park model[3] and the eddy viscosity model.[4] These models provide a quick, preliminary description of the wake interactions in a wind farm. Several high fidelity CFD models have been developed as well.[5,6] These high fidelity models are more

*Graduate Student, Department of Aerospace Engineering and Mechanics, anno0010@umn.edu
†Assistant Professor, Department of Aerospace Engineering and Mechanics
‡Assistant Professor, Department of Aerospace Engineering and Mechanics

accurate tools and can be used for evaluating wind farm controllers. However, they are computationally expensive. These low- and high-fidelity models have been used to evaluate wind farm control strategies. The analysis provides conflicting results based on the wake model chosen for control design. For example, control strategies designed using simple static models often report significant improvements in wind farm performance.[2] However, an analysis of such control strategies using high fidelity simulations results in minimal to no improvements in wind farm performance.

Improving models for wind farm control requires a better understanding of the aerodynamic interactions in a wind farm. Techniques developed by the fluids and controls communities are both relevant for this task. First, some studies have been done to understand the dominant turbulent structures generated in CFD simulations and in experiments.[7] Proper orthogonal decomposition (POD) and dynamic mode decomposition (DMD) are two popular techniques in the fluids literature that compute the dominant modes of the flow. These modes have been used to construct reduced-order models that can be used for control, such as balanced POD and DMD with controls.[8–11] Some of these methods require computing the adjoint of system, which is not readily available in most CFD codes and is not available during experiments. The controls/system identification has an alternative set of techniques to identify models from input/output data, e.g. subspace identification techniques such as N4SID.[12] The methods generate reduced-order black box models to represent the input/output measurements from the system. In this framework the states have no physical meaning.

This paper formulates a new technique to construct a reduced-order model from simulations or experiments using an extension of DMD. The model reduction approach has two main advantages. First, it relies on input/output data from a forced response and does not require the construction/simulation of the system adjoint. Second, the reduced-order model is constructed in a way that retains the physical meaning of the states. In other words, the reduced order state can be mapped back to approximate the full-order state of the system. The method addressed in this paper projects the states onto a reduced order subspace using the dominant modes of the system and then uses direct N4SID to define the reduced-order dynamic model of the system. For simplicity, this paper will use a medium-fidelity model, described in Section II, to highlight some of the advantages of this approach with the intention of extending this work to high-fidelity models in future work. Section III reviews POD and balanced POD (BPOD), a popular method for constructing reduced-order models in the fluids literature. In addition, this section addresses standard DMD that focuses on identifying dominant spatial and temporal modes in the flow of autonomous systems. The main contribution of this paper is extending DMD to include inputs and outputs and can be used to construct a low-order model that approximates the dynamics and input/output characteristics of a wind farm. The results of this low-order model are presented in Section IV. Specifically, BPOD and DMD with inputs and outputs are compared and advantages/limiatations are addressed. Finally, conclusions and suggestions for future work are given in Section V.

II. Problem Formulation

A. Wind farm modeling

Consider a wind farm with N_{turb} number of turbines located on an arbitrary grid with arbitrary locations defined by (x_i, y_i) where i refers to the turbine i in the wind farm. Each turbine has an input axial induction factor, a_i. The axial induction for a single turbine is defined as $a_i := 1 - \frac{u_i}{U_{in}}$, where u_i denotes the average horizontal speed across the rotor plane of turbine i, and U_{in} denotes the average inflow velocity. In addition, the power of each turbine can be measured, P_i. The power generated by each turbine depends on the inflow wind speed as well as the axial induction factor. The power captured from turbine i, P_i $[W]$, is given by:

$$P_i = \frac{1}{2}\rho A u_i^3 C_{P,i} \tag{1}$$

where ρ [kg/m^3] is the air density, A [m] is the area swept by the rotor, u_i [m/s] is the wind speed perpendicular to the rotor plane, and $C_{P,i}$ is the power coefficient, which is a function of the axial induction factor:[13]

$$C_{P,i} = 4a_i(1 - a_i)^2 \tag{2}$$

Individual turbines typically try to maximize their own power by operating at an optimal axial induction factor. The optimal induction factor corresponding to the optimal power coefficient for a single turbine is

$a = \frac{1}{3}$. See additional details and references on single turbine control.[13]

The turbines operating at the front of the wind farm disturb the flow through the wind farm and this impacts turbines operating downstream. The wind farm control problem can be thought of as a multi-input, multi-output system where the axial induction factors at each turbine would be the actuator inputs and the power measured at each turbine would be the outputs. By properly coordinating the turbines in a wind farm, there is the potential to maximize power and reduce overall structural loads. A few control strategies have been investigated in the literature including yaw control and axial-induction-based control.[2,14] This paper specifically focuses on axial-induction-based control. Section IV.B briefly outlines axial-induction-based control. However, the main contribution of this paper is in the development of an accurate reduced-order model.

B. Governing Equations

The actuator disk model is considered in this paper.[15,16] This model solves the 2D unsteady, incompressible, Navier-Stokes equations. The typical operating wind speeds in a wind farm do not exceed 25 m/s. This is low relative to the speed of sound at sea level ($\sim$300 m/s) and hence it is sufficient to assume incompressibility.[17] Let (u, v) denote the streamwise and spanwise velocity components and (x, y) denote the downstream and spanwise distances. Under these assumptions, the dynamics for (u, v) are governed by the following partial differential equations:

$$\frac{\partial u}{\partial x} + \frac{\partial v}{\partial y} = 0 \tag{3}$$

$$\frac{\partial u}{\partial t} + u\frac{\partial u}{\partial x} + v\frac{\partial u}{\partial y} = -\frac{1}{\rho}\frac{\partial P}{\partial x} + \nu\left(\frac{\partial^2 u}{\partial x^2} + \frac{\partial^2 u}{\partial y^2}\right) + f_x \tag{4}$$

$$\frac{\partial v}{\partial t} + u\frac{\partial v}{\partial x} + v\frac{\partial v}{\partial y} = -\frac{1}{\rho}\frac{\partial P}{\partial y} + \nu\left(\frac{\partial^2 v}{\partial x^2} + \frac{\partial^2 v}{\partial y^2}\right) \tag{5}$$

where ν [m^2/s] is the kinematic viscosity and f_x [N/m^3] is a volume force on the N_{turb} turbines in the x direction. The loading of each turbine is defined linearly. Specifically, assume that all spatial units have been nondimensionalized by the turbine diameter D. If the hub of the upstream turbine i is placed at $x = x_i$ and $y = y_i$ then the rotor plane lies within $y_i - \frac{1}{2} \leq y \leq y_i + \frac{1}{2}$. The forcing term introduced by the turbines is then given by:

$$f_x(x, y, t) := \begin{cases} kC_{T,i}(t)|y - y_i| & \text{if } x = x_i \ \& \ |y - y_i| \leq 0.5 \\ 0 & \text{else} \end{cases} \tag{6}$$

where $k := \rho A U_{in}^2$ and $C_{T,i}$ is the thrust coefficient of the turbine i. The thrust coefficient for each turbine is a function of the axial induction factor and is defined as $C_{T,i}(t) = 4a_i(t)(1 - a_i(t))$ where $a_i(t)$ is the time varying single input to the turbine i. This linear profile is smallest at the rotor hub and grows linearly at the blade tips. The loading magnitude, as specified by the input $a_i(t)$, can be changed on a real turbine via blade pitch or changing the tip speed ratio via generator torque control.[13,18]

These equations are solved using standard CFD methods.[19] Specifically, a central differencing scheme was used for the 2D actuator disk model. The grid is defined by N_x points in the streamwise x direction and N_y point in the spanwise y direction. For this actuator disk model, the typical spacing between grid points is $\delta x = 0.05$ and $\delta y = 0.05$ with a typical time step of $\delta t = 0.01$. Fig. 1a and 1b show an example of a 4×4 wind farm where mean streamwise and spanwise velocity are computed for the actuator disk model. In these figures, the turbines are separated by $3D$ in the spanwise y direction and $4D$ in the streamwise x direction. The velocities are normalized by U_∞.

The boundary conditions of this model are:

$$\begin{aligned} u(x = 0, y, t) = u(x, y = 0, t) = u(x, y = L, t) = U_\infty \\ v(x = 0, y, t) = v(x, y = 0, t) = v(x, y = L, t) = 0 \end{aligned} \tag{7}$$

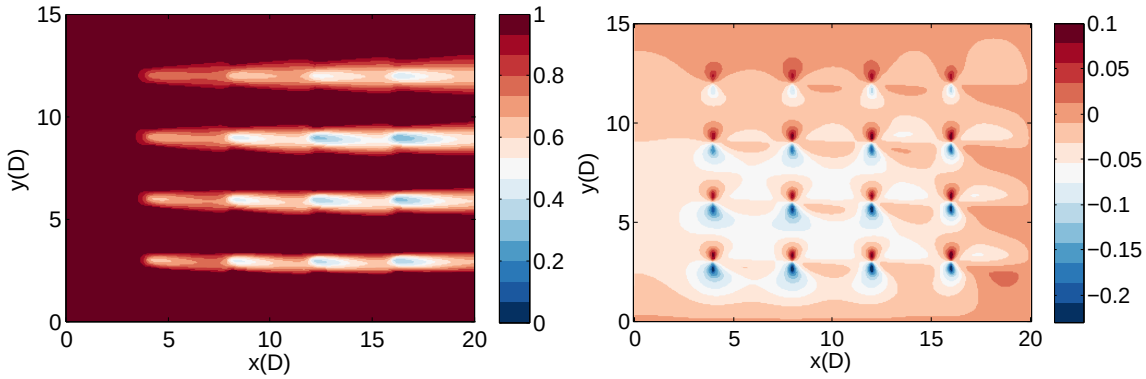

Figure 1. Mean streamwise (left) and spanwise (right) velocity computed using the actuator disk model for a 4×4 wind farm with $3D$ spacing in the y direciton and $4D$ spacing in the x direction

where L is the total spanwise distance. In this example, $L = 15D$, the streamwise distance is $20D$, $Nx = 401$, $Ny = 301$, the kinematic viscosity is $\nu = 1.461 \times 10^{-2}$ m^2/s, and $U_\infty = 8$ m/s. This would amount to 240,000 states for this particular example by having 2 states (u, v) per grid point. More realistic, higher fidelity codes will have even larger state dimensions. Note that the viscosity is significantly larger than the typical kinematic viscosity of air. This leads to a small Reynolds number, approximately 100, which is not realistic in wind farms. However, for the purposes of this paper, we are restricting our flow to a low Reynolds number to demonstrate the feasibility of the reduced-order modeling approach proposed in this paper. Future work will include simulating wind farms with the appropriate Reynolds number, approximately 10^6.

Note the turbines are modeled as actuator disks. The wakes directly behind real turbines are dominated by tip vortices that are generated based on the blade geometry. The blades are not modeled in this simulation and as a result, this model cannot accurately depict this near wake region. However, this model captures the effects of the flow far downstream, greater than $3D$, where the flow is less dependent on turbine geometry. Therefore, this model is useful for studying the far wake of a turbine in steady and unsteady flows. It should be noted that changing wind speed and direction are not addressed in this paper. It is envisioned that these issues could be handled via parameter varying models, i.e. models are constructed at each operating condition and then stitched together. Additional work is being done in this area and this would enable the design of gain-scheduled controllers in a similar manner as done at the single turbine level.[20]

C. Linearized Equations

The first step in producing a model suitable for controls is to linearize the equations of the actuator disk model. For the purposes of this paper, the actuator disk equations will be linearized around a base flow of $\mathbf{U} = (U(x, y), V(x, y))$ where $U(x, y)$ and $V(x, y)$ define the baseflow that corresponds to all turbines operating at their peak efficiency.

The linearized governing equations about the baseflow, after some algebraic manipulation, can be rewritten as:

$$\frac{d}{dt}\begin{bmatrix} u' \\ v' \end{bmatrix} = A \begin{bmatrix} u' \\ v' \end{bmatrix} + Ba(t) \tag{8}$$

where $u' \in \mathbb{R}^{(N_x N_y) \times 1}$ denotes the fluctuations from the baseflow in the streamwise direction, $v' \in \mathbb{R}^{(N_x N_y) \times 1}$ denotes the fluctuations from the baseflow in the spanwise direction, $A \in \mathbb{R}^{(2 \times N_x N_y) \times (2 \times N_x N_y)}$ contains the spatial discretization information of the flow field, $B \in \mathbb{R}^{(2 \times N_x N_y) \times N_{turb}}$ contains the location of the turbines, and $a(t) \in \mathbb{R}^{N_{turb} \times 1}$ is the input to the turbines with N_{turb} denoting the number of inputs, which in this case is the number of turbines.

The wind farm output is the vector of all power produced by all turbines denotes $P \in \mathbb{R}^{N_{turb}}$. Recall that the power P_i produced by turbine i is given in (1). Linearizing (1) for each turbine yields the following measurement equation:

$$P = \begin{bmatrix} C & 0 \end{bmatrix} \begin{bmatrix} u' \\ v' \end{bmatrix} + Da(t) \tag{9}$$

where $C \in \mathbb{R}^{N_{turb} \times (N_x N_y)}$ contains the locations of the measurements with N_{turb} number of outputs, and $D \in \mathbb{R}^{N_{turb} \times N_{turb}}$ contains information about the turbine efficiency. More details on the linearization can be found in Schmid et. al.[21] In this representation, the linearized system is given by a dynamic system of the form:

$$\begin{aligned} \dot{x} &= Ax + Ba \\ y &= Cx + Da \end{aligned} \tag{10}$$

where $x := \begin{bmatrix} u' \\ v' \end{bmatrix}$. This linearized model contains $2 \times N_x N_y$ states and is not suitable for control design and analysis. The model reduction techniques described in the next section can be used to obtain a low-order model of the wind farm.

III. Reduced-order modeling

The following subsections briefly summarizes several existing techniques for reduced-order modeling. These are used for comparison with the proposed Inputs/Outputs DMD technique.

A. Balanced Truncation

A standard model reduction approach is balanced truncation.[22–24] Consider the linearized actuator disk model (10). To perform balanced truncation on this problem, the controllability and observability Gramians need to be computed to understand the influence of the states on the inputs and outputs of the system. Specifically, the controllability Gramian specifies the minimum control energy required to reach any specific state. States that require less energy to reach are more controllable and hence have a greater influence on the input/output dynamics. Similarly, the observability Gramian specifies the energy in the output measurement when the system evolves from a given initial state (with zero input). States that produce more energy in the output are more observable and hence have a greater influence on the input/output dynamics. The Gramians can be computed by solving the Lyapunov equations:

$$\begin{aligned} AW_c + W_c A^* + BB^* &= 0 \\ A^* W_o + W_o A + C^* C &= 0 \end{aligned} \tag{11}$$

where W_c is the controllability Gramian and W_o is the observability Gramian.

The Gramians are defined by specific coordinates. These coordinates define in which directions the strongest states are aligned. The controllability and observability Gramians can have different coordinates. This makes it difficult to choose states to retain since a state may be strongly observable, but not controllable and vice versa. A transformation can be applied to align the properties of the controllability and observability Gramians, which allows you to retain states that are strongly controllable and/or observable. A coordinate transformation T can be constructed to diagonalize both the controllability and observability Gramians:

$$T^{-1} W_c (T^{-1})^* = T^* W_o T = \Sigma = diag(\sigma_1, ..., \sigma_n) \tag{12}$$

where σ are the Hankel singular values that are independent of the coordinate transformation. Under this transformed system, the states that are significantly influenced by the inputs are also the states that have a significant impact on the outputs. However, this approach becomes intractable for large systems (state dimension larger than 1000) as it requires the solution of the two Lyapunov equations (11). See additional details.[24, 25]

B. Proper Orthogonal Decomposition

Proper orthogonal decomposition (POD) provides a low-order approximation that is capable of capturing the dominant turbulent structures in the flow. Specifically, POD can be used to extract dominant spatial features from both simulation and experimental data that can be used to dynamically reconstruct the structures in a flow field.[26] This can be done by projecting the velocity field on to a set of orthogonal basis functions. A projection matrix is constructed to minimize the error between the evolving state $x(t)$ and a low-order projection:

$$\int_0^{T_{max}} \|x(t) - P_r x(t)\|^2 \, dt \tag{13}$$

where T_{max} is the total simulation time, $x(t)$ is the simulated variable, and P_r is the projection matrix. The projection matrix can be defined in terms of the basis functions:

$$P_r = \sum_{k=1}^{r} \varphi_k \varphi_k^* \tag{14}$$

where φ_k are the POD modes and r represents the reduced order of the system. The eigenfunctions of the flow field are shown to produce the optimal projection that minimizes the total error between the full system and the reduced order system.[8,9,26,27]

The POD modes of the flow can be computed from the snapshots of the nonlinear system, $x(t)$. A data matrix of the snapshots is formed by $X_0 = [x(t_1), x(t_2), ..., x(t_m)]$ where m is the number of snapshots. The POD modes are then computed by taking the singular-value decomposition of the data matrix, i.e. $X_0 = U\Sigma V^T$. The POD modes are contained in U. **Transition sentence is needed here**

POD modes are good at representing specific datasets. However, POD modes do not necessarily provide a good description of a dynamically evolving flow driven by a forcing input.

Balanced Proper Orthogonal Decomposition

The combination of POD modes and balanced truncation can be used to implement a method known as balanced proper orthogonal decomposition (BPOD).[8,9,27] Consider the linearized actuator disk system (10). The solution $x(t)$ is found by solving $\dot{x} = Ax$ where the inputs have been set to 0. The initial conditions are defined as the columns of B. One simulation needs to be run for each input. This system will be referred to as the forward system for the remainder of this paper.

In addition to computing the solution for the forward system, the solution to the adjoint system can be found by integrating the system:

$$\dot{z} = A^* z \tag{15}$$

with the initial conditions defined as the columns of C^T. As with the forward system, one simulation needs to be run for each output. Physically, the adjoint system is used to evaluate the sensitivity of the system due to some perturbation.[28–31]

Using the solutions, $x(t)$ and $z(t)$, the data matrices are formed with the snapshots gathered in the simulations.

$$\begin{aligned} X &= [x_1(t_1), ..., x_1(t_m), ..., x_p(t_1), ..., x_p(t_m)] \\ Y &= [z_1(t_1), ..., z_1(t_m), ..., z_p(t_1), ..., z_q(t_m)] \end{aligned} \tag{16}$$

where m is the number of snapshots, p is the number of inputs, and q is the number of outputs. At this point, the BPOD modes can be computed from the singular value decomposition of Y^*X:

$$Y^*X = \begin{bmatrix} U_1 & U_2 \end{bmatrix} \begin{bmatrix} \Sigma_1 & 0 \\ 0 & \Sigma_2 \end{bmatrix} \begin{bmatrix} V_1 \\ V_2 \end{bmatrix} \tag{17}$$

where Σ_1 is a matrix $(r \times r)$ and r is the reduced order of the system. The transformation matrices, T and S, can be defined as:

$$
\begin{aligned}
T &= XV_1\Sigma_1^{-\frac{1}{2}} \\
S &= \Sigma_1^{-\frac{1}{2}}U_1^*Y^*
\end{aligned}
\tag{18}
$$

The reduced order system is now:

$$
\begin{aligned}
\dot{x}_r &= SATx + SBf \\
y &= CT
\end{aligned}
\tag{19}
$$

Note that for a SIS system, the X and Y matrices are $n \times m$ matrices where n is the state dimension, which is typically very large, i.e. tens of thousands or more, while m is the number of snapshots, which is typically on the order of hundreds. The Lyapunov equations in (11) are of dimension n and directly solving these equations is prohibitive as solving a Lyapunov equation scales with $O(n^3)$.[32] The product of Y^*X requires $O(m^2n)$ operations which scales linearly in n. The resulting matrix is only $m \times m$ and hence the singular value decomposition in (17) can be performed at a reasonable computational cost. However, a linearized simulation needs to be run for every input and the adjoint system needs to be run for every output. This is particularly an issue if you want a model where the output is the full state, i.e. $y = x$.

C. Dynamic Mode Decomposition

This section briefly reviews the use of DMD to construct reduced order dynamic models from nonlinear systems.[21] This method attempts to fit a discrete-time linear system to a set of snapshots from simulation or experiments. Consider a system modeled by the following discrete-time, nonlinear dynamics (such as the actuator disk):

$$
x_{k+1} = f(x_k) \tag{20}
$$

where $x \in \mathbb{R}^n$ is the state vector. A collection of snapshot measurements $\{x_k\}_{k=0}^m \subset \mathbb{R}^n$ is obtained for the system either via simulation or experiments.

The objective is to approximate the system on a low dimensional subspace. Assume there is a matrix A that relates the snapshots in time by:

$$
x_{k+1} = Ax_k \tag{21}
$$

The DMD method attempts to fit the snapshots in time using a low rank matrix A. DMD is different from POD in that it constructs both the low dimensional subspace as well as the model (matrix A) from the snapshot data. This can be used to construct DMD modes that correspond to specific modal frequencies.

The problem is first simplified by assuming that an r-dimensional subspace of $\mathbb{R}^n$ has been selected. An orthonormal basis for this subspace is specified by the columns of a matrix $Q \in \mathbb{R}^{n\times r}$ with $Q^TQ = I_r$. The truncated, reduced order model takes the form:

$$
z_{k+1} = (Q^TAQ)z_k := Fz_k \tag{22}
$$

The state matrix $F := Q^TAQ \in \mathbb{R}^{r\times r}$ describes the dynamics on the reduced order subspace. Solutions z_k to this reduced order model can be used to construct approximate solutions to the full order model (21) as $x_k \approx Qz_k$. This is equivalent to the following low-rank approximation for the full-order state matrix: $A \approx QFQ^T$. The reduced order state matrix, F, can be found by taking the snapshots of (21) and forming the following data matrices:

$$
X_0 = [x_1, x_2, ..., x_{m-1}] \tag{23}
$$

$$
X_1 = [x_2, x_3, ..., x_m] \tag{24}
$$

where x_k are the snapshots and m is the number of snapshots. The optimal choice for the reduced order state matrix, F, can be found by minimizing the error of the Frobenius norm.

$$\min_{F \in \mathbb{R}^{r \times r}} \|X_1 - (QFQ^T)X_0\|_F^2 \tag{25}$$

The optimal F that minimizes this least squares cost is given by:

$$F_{opt} := Q^T X_1 (Q^T X_0)^\dagger \tag{26}$$

the † denotes the pseudo-inverse.

The typical, sub-optimal choice for the projection subspace, Q, is the POD modes of X_0. Specifically, let $X_0 = U\Sigma V^T$ be the SVD of X_0. The linear system can be approximated on a subspace defined by the first r POD modes of X_0, i.e. $Q := U_r$ where U_r are the first r columns of U. The optimal reduced order state-matrix for this choice is:

$$F_{opt} := U_r^T X_1 (U_r^T X_0)^\dagger = U_r^T X_1 V_r \Sigma_r^{-1} \tag{27}$$

The corresponding low rank approximation for the full-order state matrix is

$$A \approx U_r F_{opt} U_r^T = U_r U_r^T X_1 X_0^\dagger \tag{28}$$

This model provides information about the dynamic modes of the system. Specifically, let F_{opt} have an eigenvalue decomposition $T\Lambda T^{-1}$ where T, $\Lambda \in \mathbb{C}^{r \times r}$. $\Lambda = diag(\lambda_1, \ldots, \lambda_r)$ has the (possibly complex) eigenvalues of F_{opt} on the diagonal. The matrix $T := [t_1, \ldots, t_r]$ contains the corresponding eigenvectors, i.e. $F_{opt} t_j = \lambda_j t_j$. The DMD modes are given by $\psi_j = U_r t_j$ for $j = 1, \ldots, r$. Equation 28 and the eigenvalue relation $F_{opt} t_j = \lambda_j t_j$ imply that $A\psi_j = \lambda_j \psi_j$. Thus these modes have the property that if $x_0 = \psi_j$ then $x_k = \lambda_j^k \psi_j$ for $k = 0, 1, \ldots$. In other words, each mode ψ_j provides spatial information regarding a specific temporal frequency λ_j for the system.

One limitation of this approach is that it cannot produce input/output models. For example, the dynamics and the modes will be disrupted by external forcing, i.e. DMD is not robust to perturbations in the system.

D. Inputs/Outputs DMD

An extension of the DMD approach is made here to include inputs and outputs. DMD has previously been looked at in the context of control.[11] This approach projects the full-order model onto the output subspace. By using the output subspace, the inputs are accounted for when fitting the data to a linear system. The approach specified in this paper combines DMD with standard subspace ID,[12] often used in the control literature, to constrict an input/output model suitable for control. This Inputs/Outputs DMD implementation will be referred to as IODMD for the remainder of the paper. Again, consider a discrete-time nonlinear system:

$$\begin{aligned} x_{k+1} &= f(x_k, u_k) \\ y_k &= h(x_k, u_k) \end{aligned} \tag{29}$$

where $x \in \mathbb{R}^n$, $u \in \mathbb{R}^{n_u}$, and $y \in \mathbb{R}^{n_y}$ are the state, input, and output vectors. Assume that the system has an equilibrium condition described by $(\bar{x}, \bar{u}, \bar{y})$ such that

$$\bar{x} = f(\bar{x}, \bar{u}) \tag{30}$$

$$\bar{y} = h(\bar{x}, \bar{u}) \tag{31}$$

If the state is initialized at $x_0 = \bar{x}$ and the input is held fixed at $u_k = \bar{u}$ for $k = 0, 1, \ldots$ then the state will remain in equilibrium at $x_k = \bar{x}$ for $k = 0, 1, \ldots$. In addition, the output will remain at $y_k = \bar{y}$ for $k = 0, 1, \ldots$. A collection of snapshot measurements are obtained via simulation or experiments by exciting the system near this equilibrium point. The snapshots include measurements of the state $\{x_k\}_{k=0}^m \subset \mathbb{R}^n$, input $\{u_k\}_{k=0}^m \subset \mathbb{R}^{n_u}$, and output $\{y_k\}_{k=0}^m \subset \mathbb{R}^{n_y}$. Define perturbations of these measurements from the equilibrium condition:

$$\delta x_{k+1} := x_{k+1} - \bar{x} \tag{32}$$

$$\delta u_{k+1} := u_{k+1} - \bar{u} \tag{33}$$

$$\delta y_{k+1} := y_{k+1} - \bar{y} \tag{34}$$

The proposed IODMD attempts to fit the snapshot measurements in time by:

$$\begin{aligned} \delta x_{k+1} &= A\delta x_k + B\delta u_k \\ \delta y_k &= C\delta x_k + D\delta u_k \end{aligned} \tag{35}$$

The state matrices (A, B, C, D) are real matrices with dimensions compatible to those of (x, u, y). The intent is to apply the method for systems where the state dimension is extremely large ($n > 10000$) but with moderate input and ouptut dimensions (n_u, $n_y < 100$). The state is projected onto a low dimensional subspace in order to make the computations tractable.

Similar to standard DMD, the problem is first simplified by assuming that an r-dimensional subspace of $\mathbb{R}^n$ has been selected. An orthonormal basis for this subspace is specified by the columns of a matrix $Q \in \mathbb{R}^{n\times r}$ with $Q^TQ = I_r$. As in the previous section, the state can be projected onto the subspace defined by Q. This yields a reduced order state $z := Q^T\delta x \in \mathbb{R}^r$. A truncated model can be expressed in terms of this reduced-order state:

$$\begin{aligned} z_{k+1} &= (Q^TAQ)z_k + (Q^TB)\delta u_k := Fz_k + G\delta u_k \\ \delta y_k &= (CQ)z_k + D\delta u_k := Hz_k + D\delta u_k \end{aligned} \tag{36}$$

The state matrices of the reduced order system have dimensions $F \in \mathbb{R}^{r\times r}$, $G \in \mathbb{R}^{r\times n_u}$, and $H \in \mathbb{R}^{n_y\times r}$. The form of (36) is equivalent to the following low rank approximations for the full order state matrices:

$$\begin{bmatrix} A & B \\ C & D \end{bmatrix} \approx \begin{bmatrix} QFQ^T & QG \\ HQ^T & D \end{bmatrix} = \begin{bmatrix} Q & 0 \\ 0 & I_{n_y} \end{bmatrix} \begin{bmatrix} F & G \\ H & D \end{bmatrix} \begin{bmatrix} Q^T & 0 \\ 0 & I_{n_u} \end{bmatrix} \tag{37}$$

The optimal choice for the reduced order state matrices (F, G, H, D) given a specific subspace is spanned by Q. Snapshots are taken from the nonlinear system (29) and the states, inputs, and outputs are recorded as:

$$X_0 = [x_1, x_2, ..., x_{m-1}] \tag{38}$$

$$X_1 = [x_2, x_3, ..., x_m] \tag{39}$$

$$U_0 = [u_1, u_2, ..., u_{m-1}] \tag{40}$$

$$Y_0 = = [y_1, y_2, ..., y_{m-1}] \tag{41}$$

The optimal (reduced-order) state matrices are obtained by least squares. This is the direct N4SID subspace method for estimating state matrices given measurements of the (reduced-order) state, input, and output. Again, a sub-optimal, but useful, choice for the projection space is given by the POD modes of X_0. Specifically, let the SVD of X_0 be given by $X_0 = U\Sigma V^T$. The state of the linear system can be approximated on a subspace defined by the first r POD modes of X_0, i.e. $Q := U_r$. The optimal reduced order state-matrices for this choice is:

$$\begin{bmatrix} F & G \\ H & D \end{bmatrix}_{opt} = \begin{bmatrix} U_r^TX_1 \\ Y_0 \end{bmatrix} \begin{bmatrix} \Sigma_r V_r \\ U_0 \end{bmatrix}^\dagger \tag{42}$$

As with standard DMD, an eigenvalue decomposition of F_{opt} can be used to construct DMD modes that provide spatial modes associated with a specific temporal frequency for the system. This new methodology also yields input/output information for the model. This proposed method is a tractable implementation of the existing direct N4SID (subspace) method that can be applied for very large systems. This is not simply a black-box (input-output) approach because the state of the reduced order system z_k can be used to approximately reconstruct the full order state by $\delta x_k \approx U_r z_k$. Moreover, the approach only requires input/output/state data from the model. Construction and simulation of an adjoint system, as in balanced POD, is not required. Finally, the pseudo-inverse and matrix multiplications in (42) are tractable even if ~ 1000 modes are retained. Thus (F, G, H, D) can be computed retaining many modes (possibly as many modes as there are snapshots) and then standard balanced truncation can be used to reduce down to a small number of modes.

IV. Example: Wind Farm Control with Two Turbine Array

The results section of this paper focuses on obtaining a low-order model for a two-turbine array shown in Fig. 2a. The dynamic system (10) becomes a single-input-single-output system. In this two-turbine example, the downstream turbine is held constant at an optimal operating point. The single input in this scenario is the axial induction factor of the upstream turbine. The single output is the power measured at the downstream turbine. Fig. 2b shows computed mean streamwise velocity. The turbines are located at $5D$ and $10D$. The simulation used $N_x = 300$ points between $[0, 15D]$ in the streamwise x direction and $N_y = 100$ points between $[0, 5D]$ in the spanwise y direction. This yields a total of 30,000 grid points with two velocities (u, v) defined at every point resulting in 60,000 states. The simulation is run for 10 s and has a time step of 0.01 s. A direct application of the standard balanced truncation technique requires the solution of the Lyapunov equations in (11). This is computationally intractable for this system. IODMD is implemented to obtain a reduced order model that retains the input/output behavior of the system.

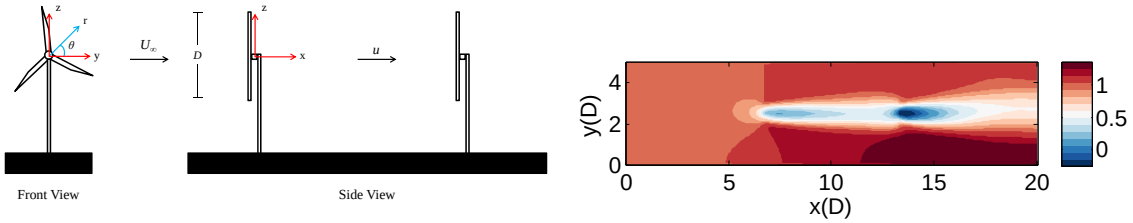

Figure 2. Left: Two-turbine setup. Right: Mean streamwise velocity computed using the actuator disk model

The remainder of this section focuses on formulating low-order models using BPOD and IODMD for this two-turbine SISO system. BPOD and IODMD are compared and the advantages and disadvantages are highlighted for both methods.

BPOD Implementation

The unforced linearized equations for the actuator disk model are simulated in time. The input, a, in (10) is set to zero. The initial condition is defined as the columns of B, which has the dimensions of the number of states by the number of inputs. Similarly the adjoint system is simulated using the columns of the C^T matrix as the initial condition. Because this is a single-input-single-output system, the forward and adjoint systems are only simulated once, one for each input/output. The data is collected in the X and Y matrices described in (16) and the BPOD modes are found by computing the SVD of Y^*X. The reduced-order model can be obtained using the transformation matrices, see (19).

IODMD Implementation

In contrast to the BPOD implementation, the full nonlinear system, rather than the linearized system, is simulated with some forcing input. Specifically, the nonlinear actuator disk model is simulated using a sine sweep input, a, to the front turbine. This input will vary the thrust the front turbine exerts on the flow. Fig. 3 shows the computed POD modes for the nonlinear actuator disk model. Note that modes 1 and 2 capture the low frequency, high energy structures in the model. The velocities are normalized by U_∞. Physically, when considering the flow behind the turbine, the lower POD modes correspond to larger frequency events such as large eddies generated in the wake of the turbine.

Comparison of BPOD and IODMD

Fig. 4a and 4b show the frequency response of the full order actuator disk model and the frequency response of the reduced order model constructed using BPOD and IODMD. Specifically, Fig. 4a shows the frequency response of the system using 1000 snapshots with IODMD. All 1000 modes are retained in this case, while only 10 modes are retained in BPOD. As mentioned previously, the reduced-order model obtained from IODMD can have many modes and then standard balanced truncation can be used to reduce the model

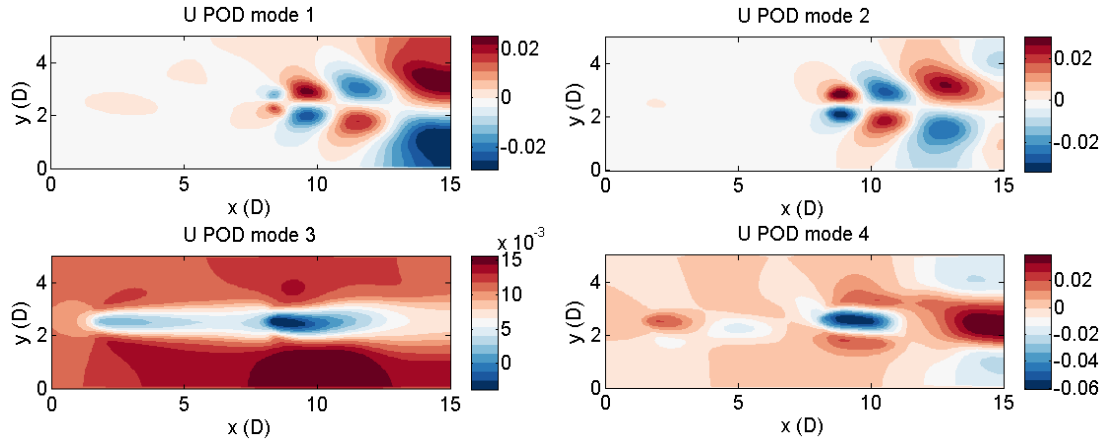

Figure 3. First four POD modes of the actuator disk model.

down to a lower order. In this case, Fig. 4b shows the 1000 state IODMD model in Fig. 4a reduced to 10 states with balanced truncation in Fig. 4b. This is in good agreement with BPOD.

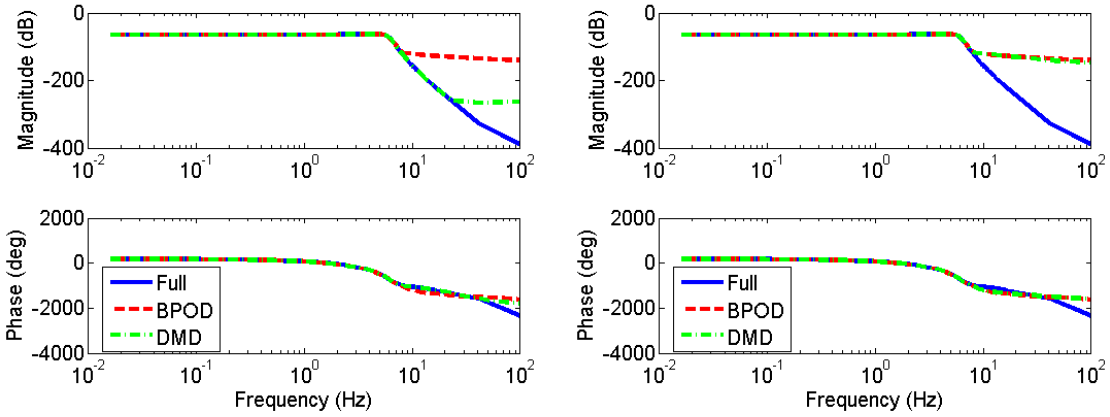

Figure 4. Frequency response of IODMD compared to BPOD and the full order system. Left: IODMD using 1000 snapshots and retaining 1000 modes. Right: IODMD applying balanced truncation to reduce the model to 10 states.

Note, there is a small, but noticeable mismatch between the reduced order models and the full order model at frequencies below 0.2 Hz in both Fig. 4a and 4b. The accuracy of the reduced order models at these low frequencies can be improved by increasing the simulated time T_{max}. Specifically, these snapshots are collected over a certain time interval $[0, T_{max}]$. Thus very low frequencies are not captured by these snapshots, i.e. roughly frequencies below $\frac{1}{T_{max}}$ rad/s are not captured in the BPOD snapshots. The simulated time in this example is 10s. In addition, the sampling of snapshots from the simulation limits the high frequency component of the reduced order model. For this case, the sampling frequency was 10^{-2} and 100 Hz is the highest frequency this model can capture. Thus the reduced order model provides a good input/output model for frequencies in this middle band.

The two methods match the full order linear model up until the upper frequency bound. The advantage of IODMD is that there is no need to compute the adjoint. In addition, the states of the reduced-order model can be used to compute the full state at a given time. Typical subspace identification methods, such as N4SID, construct a black-box input/output model where the states lack physical meaning. This new methodology addresses some of the limitations of BPOD and subspace ID to produce a reduced-order model of the fluids system that can be used for control.

V. Conclusion

This paper used a new technique of IODMD to construct a low-order model that can be used for wind farm control design and analysis. This approach takes advantage of characterizing the dominant dynamics in the flow and provides a low-order approximation of the flow. Using this low-order approximation, a reduced order model can be constructed that retains the input-to-output behavior seen in the full order model. This reduced order model has a low computational intensity and contains the necessary dynamics that are important for wind farm control. This new technique avoids computing the adjoint as is done in BPOD and the states of the reduced order model maintain some physical meaning.

Future work includes extending this model reduction technique to high-fidelity models, such as large-eddy simulations. In addition, preliminary wind farm controllers will be developed using these low-order models and validated in high-fidelity simulations and field tests. Preliminary wind farm controllers will be presented in the final version of this paper.

Acknowledgements

This work was supported by the National Science Foundation under Grant No. NSF-CMMI-1254129 entitled CAREER: Probablistic Tools for High Reliability Monitoring and Control od Wind Farms. Any opinions, findings, and conclusions or recommendations expressed in this material are those of the authors and do not necessarily reflect the views of the NSF. In addition, the authors acknowledge the support from the Institute on the Environment, University of Minnesota (Initiative for Renewable Energy and the Environment).

References

[1]Wiser, R., "Renewable Portfolio Standards in the United States - A Status Report with Data Through 2007," LBNL-154E, Lawrence Berkeley National Laboratory, 2008.

[2]Johnson, K. E. and Thomas, N., "Wind farm control: Addressing the aerodynamic interaction among wind turbines," *American Control Conference*, 2009, pp. 2104–2109.

[3]Jensen, N. O., "A note on wind generator interaction," Tech. Rep. Risø-M-2411, Risø, 1983.

[4]Ainslie, J. F., "Calculating the flowfield in the wake of wind turbines," *Journal of Wind Engineering and Industrial Aerodynamics*, Vol. 27, No. 1, 1988, pp. 213–224.

[5]Churchfield, M. and Lee, S., "NWTC design codes-SOWFA," *http://wind.nrel.gov/designcodes/simulators/SOWFA*, 2012.

[6]Yang, X., Sotiropoulos, F., Conzemius, R. J., Wachtler, J. N., and Strong, M. B., "Large-eddy simulation of turbulent flow past wind turbines/farms: the Virtual Wind Simulator (VWiS)," *Wind Energy*, 2014.

[7]Bastine, D., Witha, B., Wächter, M., and Peinke, J., "Towards a Simplified Dynamic Wake Model using POD Analysis," *arXiv preprint arXiv:1409.1150*, 2014.

[8]Willcox, K. and Peraire, J., "Balanced model reduction via the proper orthogonal decomposition," *AIAA journal*, Vol. 40, No. 11, 2002, pp. 2323–2330.

[9]Rowley, C., "Model reduction for fluids, using balanced proper orthogonal decomposition," *International Journal of Bifurcation and Chaos*, Vol. 15, No. 03, 2005, pp. 997–1013.

[10]Balajewicz, M., *A New Approach to Model Order Reduction of the Navier-Stokes Equations*, Ph.D. thesis, Duke University, 2012.

[11]Proctor, J. L., Brunton, S. L., and Kutz, J. N., "Dynamic mode decomposition with control," *arXiv preprint arXiv:1409.6358*, 2014.

[12]Viberg, M., "Subspace-based methods for the identification of linear time-invariant systems," *Automatica*, Vol. 31, No. 12, 1995, pp. 1835–1851.

[13]Burton, T., Jenkins, N., Sharpe, D., and Bossanyi, E., *Wind energy handbook*, John Wiley & Sons, 2011.

[14]Fleming, P. A., Gebraad, P. M., Lee, S., van Wingerden, J.-W., Johnson, K., Churchfield, M., Michalakes, J., Spalart, P., and Moriarty, P., "Evaluating techniques for redirecting turbine wakes using SOWFA," *Renewable Energy*, Vol. 70, 2014, pp. 211–218.

[15]Sørensen, J. N. and Myken, A., "Unsteady actuator disc model for horizontal axis wind turbines," *Journal of Wind Engineering and Industrial Aerodynamics*, Vol. 39, No. 1, 1992, pp. 139–149.

[16]Sørensen, J. N. and Kock, C. W., "A model for unsteady rotor aerodynamics," *Journal of wind engineering and industrial aerodynamics*, Vol. 58, No. 3, 1995, pp. 259–275.

[17]Schlichting, H., Gersten, K., and Gersten, K., *Boundary-layer theory*, Springer Science & Business Media, 2000.

[18]Johnson, K. E., Pao, L. Y., Balas, M. J., and Fingersh, L. J., "Control of variable-speed wind turbines: standard and adaptive techniques for maximizing energy capture," *Control Systems, IEEE*, Vol. 26, No. 3, 2006, pp. 70–81.

[19]Zikanov, O., *Essential computational fluid dynamics*, John Wiley & Sons, 2010.

[20]Wang, S. and Seiler, P., "Gain scheduled active power control for wind turbines," *AIAA Atmospheric Flight Mechanics Conference*, 2014.

[21]Schmid, P. J. and Henningson, D. S., *Stability and transition in shear flows*, Vol. 142, Springer, 2001.

[22]Moore, B., "Principal component analysis in linear systems: Controllability, observability, and model reduction," *Automatic Control, IEEE Transactions on*, Vol. 26, No. 1, 1981, pp. 17–32.

[23]Pernebo, L. and Silverman, L., "Model reduction via balanced state space representations," *Automatic Control, IEEE Transactions on*, Vol. 27, No. 2, 1982, pp. 382–387.

[24]Enns, D. F., "Model reduction with balanced realizations: An error bound and a frequency weighted generalization," *Decision and Control, 1984. The 23rd IEEE Conference on*, Vol. 23, IEEE, 1984, pp. 127–132.

[25]Skogestad, S. and Postlethwaite, I., *Multivariable feedback control: analysis and design*, Vol. 2, Wiley New York, 2007.

[26]Holmes, P., Lumley, J. L., and Berkooz, G., *Turbulence, coherent structures, dynamical systems and symmetry*, Cambridge university press, 1998.

[27]Lall, S., Marsden, J. E., and Glavaški, S., "A subspace approach to balanced truncation for model reduction of nonlinear control systems," *International journal of robust and nonlinear control*, Vol. 12, No. 6, 2002, pp. 519–535.

[28]Jameson, A., "Aerodynamic shape optimization using the adjoint method," *Lectures at the Von Karman Institute, Brussels*, 2003.

[29]Giles, M. B. and Pierce, N. A., "An introduction to the adjoint approach to design," *Flow, turbulence and combustion*, Vol. 65, No. 3-4, 2000, pp. 393–415.

[30]Luchini, P. and Bottaro, A., "Adjoint equations in stability analysis," *Annual Review of Fluid Mechanics*, Vol. 46, No. 1, 2014, pp. 493.

[31]Wunsch, C., *Discrete inverse and state estimation problems: with geophysical fluid applications*, Vol. 2, Cambridge University Press Cambridge, 2006.

[32]Bartels, R. H. and Stewart, G., "Solution of the matrix equation AX+ XB= C [F4]," *Communications of the ACM*, Vol. 15, No. 9, 1972, pp. 820–826.